Journal of the Ceramic Society of Japan 121 [3] 299-302 2013 Paper

Cosolvent-free sol–gel synthesis of rare-earth and aluminum codoped monolithic silica glasses

Ken KANEKO, Koichi KAJIHARA† and Kiyoshi KANAMURA

Department of Applied Chemistry, Graduate School of Urban Environmental Sciences, Tokyo Metropolitan University, 1–1 Minami-Osawa, Hachioji, Tokyo 192–0397, Japan

A cosolvent-free sol–gel method to synthesize monolithic silica glasses containing both of rare-earth and aluminum ions has been studied. Fracture during drying and bloating during sintering are significantly suppressed by forming macroporous wet gels via macroscopic phase separation in parallel with gelation. The resultant rare-earth and aluminum codoped silica glasses exhibit good visible transparency, suggesting an improvement of dispersion of rare-earth ions in these glasses. The aluminum codoping increases the photoluminescence efficiency in glasses doped with Nd^{3+} ions.

Key-words : Sol–gel method, Silica glass, Rare-earth aluminum codoping

[Received October 1, 2012; Accepted December 15, 2012]

1. Introduction

Silica glass is an important amorphous optical material because of its excellent transparency over wide spectral region, good shape workability, and good mechanical and chemical properties. Rare-earth (RE) doped silica glasses utilize these properties and are used as active gain media of solid-state lasers, fiber amplifiers, and phosphors.[1),2)] However, the solubility of RE ions in silica glasses is relatively low, and doping of RE ions at high concentrations often causes aggregation of RE ions and crystallization, leading to degradation of transparency and photoluminescence (PL) efficiency. Aluminum (Al) is known as an element that enhances the dissolution of RE ions in silica glass.[3)–18)] Most of RE-Al codoped silica glasses for optical application have been synthesized by vapor phase methods, such as the vapor-phase axial deposition and chemical vapor deposition (CVD),[3),4),12),16)] because these methods are suitable to suppress the incorporation of metallic impurities. However, the vapor pressure of RE compounds is often low, making the direct vapor-phase loading of RE ions into silica glass difficult. Sintering of silica soots immersed in solutions of RE ions is another more common way of preparing RE-doped silica glasses, but homogeneous RE doping at high concentrations may be difficult because of the possible aggregation of RE ions at the surfaces of soots during drying and sintering.

Solution-based synthesis methods seem promising for preparation of RE-Al codoped silica glasses containing RE ions at high concentrations. For example, sol–gel method, a well-known wet chemical technique, has been employed to prepare silica glasses doped with RE ions more than 1×10^4 ppmw (1 wt % of RE_2O_3 or RE to Si molar ratio of ~0.003–0.004).[5)–7),9)–11),14),15)] However, drying of sol–gel derived silica gels is usually difficult because they contain nano- and mesopores, and the drying of the pore liquid induces a large capillary pressure to cause an uneven shrinkage and fracture.[19)] To avoid the fracture, a long processing time (~2–4 weeks) is commonly needed. Incorporation of particulate silica fillers is effective in suppressing the fracture, because the fillers strengthen the gel framework and form macropores to reduce the capillary pressure.[20)–25)] From this aspect, aluminosilicate zeolite powders are attractive not only for fillers but also for aluminum sources that can form dispersed RE-Al pairs in their cavities and channels. Large monolithic Nd–Al codoped silica glasses have been fabricated using Nd-loaded zeolite X powders.[26)] The resultant glass has a high thermal shock parameter, and its operation as a 40 J class high power laser has been demonstrated.[27)]

Here we describe another approach to prepare monolithic RE-Al codoped silica glasses. This method is based on the sol–gel synthesis of monolithic silica glasses from tetraethoxysilane (TEOS)-water binary systems, which we have developed recently.[28)–31)] The precursor solution undergoes macroscopic phase separation in parallel with gelation, and the resultant macroporus structure facilitates the drying and sintering of gels while suppressing the fracture. Furthermore, this method does not need alcohols, which have been used almost routinely as cosolvents to obtain homogeneous precursor solutions of water and alkoxides. Preparation and optical properties of Nd-doped glasses are mainly presented.

2. Experimental procedure

A dilute aqueous solution of nitric acid was added to 25 mmol (5.2 g) of TEOS (Shin-Etsu Chemical) and stirred for 120 min at 20°C in a sealed plastic container to form a clear solution with a $TEOS:H_2O:HNO_3$ molar ratio of $1:x_1:0.002$. The resultant solution was further mixed with an aqueous solution of ammonium acetate ($AcONH_4$), aluminum nitrate nonahydrate [$Al(NO_3)_3{\cdot}9H_2O$], and a RE salt to form a solution with overall composition $TEOS:H_2O:HNO_3:AcONH_4:Al(NO_3)_3:RE\ salt = 1:x_1 + x_2:0.002:y:z_{Al}:z_{RE}$, where $x_1 + x_2$ and z_{RE} were respectively fixed at 10 and 0.01 in this study. After stirring for 1 min the stir bar was removed and the solution was allowed to gel at 20°C. The resultant wet gel was aged for 1 d at 60°C. Then the solvent phase was disposed by opening the container and the gel was gently dried at 60°C. The loss of Nd^{3+} ions due to the dissolution into the disposed solvent phase was evaluated from the intensity of the $^4I_{9/2} \rightarrow {}^4G_{5/2} + {}^2G_{7/2}$ absorption bands of Nd^{3+} ions at

† Corresponding author: K. Kajihara; E-mail: kkaji@tmu.ac.jp

~580 nm using a reference solution with a H_2O:EtOH:$Nd(OAc)_3$ molar ratio of 8:4:0.01. The dried gel was sintered in a tube furnace with a heating rate of 200°C h^{-1} and maintained at the target temperature (1150–1200°C) within 0.5 h. The sintering atmosphere was switched from air to helium at 600°C. A conventional spectrometer (U-4100, Hitachi) was used to measure optical absorption spectra. Devitrification was examined by X-ray diffraction (XRD, RINT Ultima II, Rigaku). Density of the glass samples was determined using a pycnometer. The PL time decay was detected by an InGaAs PIN photodiode (G8605-23, Hamamatsu) equipped with a 1064 nm optical bandpass filter, and recorded using an oscilloscope. The excitation light from a laser diode (~1.5 W at 808 nm) was periodically cut by an optical chopper.

3. Results

In this study, neodymium acetate hydrate was used as the main RE salt. A clear solution was obtained after the second mix, and it turned to an opaque or translucent gel in ~1–2 h, typically at $x_1 \lesssim 2$. **Figure 1** shows effects of x_1 on the appearance of Nd–Al codoped dried gels prepared at $y = 0.09$ and $z_{Al} = 0.01$, and dried for ~2 weeks. The opacity, which resulted from the macroscopic phase separation into gel and solvent phases in parallel with gelation,[28)–31)] decreased with an increase in x_1. Because of the presence of the macropores, it was relatively easy to suppress the fracture, particularly at compositions with smaller x_1 values. Sintering in a helium atmosphere easily converted these macroporous dried gels to monolithic glasses, while suppressing the fracture and bloating, which are mainly associated with the dehydration from SiOH groups.[32),33)]

Figure 2 shows optical absorption spectrum of an Al-codoped glass ($z_{Al} = 0.01$) prepared at $x_1 = 1.76$ and $y = 0.09$, and an Al-free glass ($z_{Al} = 0$) prepared at $x_1 = 1.86$ and $y = 0.01$. A photograph of these glasses is also shown. The densities of the Al-free and Al-codoped glasses were ~2.25 and ~2.26 g cm^{-3}, respectively. These values agree well with the values reported previously,[4),34)] indicating that the glasses are fully densified. The transparency of the Al-codoped glass was better than that of the Al-free glass, particularly at wavelengths shorter than 500 nm. The fundamental absorption band of the SiO–H stretching mode (~3680 cm^{-1}, not shown) was too strong to be measured accurately. Thus, the concentration of SiOH groups was evaluated from the absorption coefficient of the first overtone band located at ~7250 cm^{-1}. The peak absorption cross section of the 7250 cm^{-1} band (~1.7×10^{-21} cm^2) was calculated from the peak absorption cross section of the fundamental band reported in the literature (2.9×10^{-19} cm^2 [35)]) and the ratio of the peak amplitude between the fundamental and overtone bands (~175:1). The concentrations of SiOH groups were ~2×10^{20} cm^{-3}, both in the Al-codoped and Al-free glasses.

It was found that a part of Nd^{3+} ions was lost with the disposed solvent phase after the aging. The fraction of the eluted Nd^{3+} ions was ~8 ± 8% for the Al-free sample and ~20 ± 5% for the Al-codoped sample. The reason for the increase in the loss of Nd^{3+} ions by Al codoping is currently not known. The concentration of Nd^{3+} ions corrected for the loss was ~2.0×10^{20} cm^{-3} for the Al-free glass and ~1.8×10^{20} cm^{-3} for the Al-codoped glass. It was also found that the loss of Nd^{3+} ions from the Nd–P codoped glass, which we reported previously,[31)] was ~9 ± 3% and was comparable to that of the Al-free glass.

Figure 3 shows XRD patterns of the crushed Al-free and Al-codoped glasses. A weak and broad diffraction, probably attributed to Nd_2O_3 crystallites,[14)] was observed at $2\theta \cong 30.5°$ in the Al-free glass, whereas the formation of crystalline phases was not obvious in the Al-codoped glass.

Figure 4 shows infrared PL decay curves of the $^4F_{3/2} \rightarrow {}^4I_{11/2}$ transition of Nd^{3+} ions in the Al-codoped and Al-free glasses. These PL decay curves were not single exponential. Fitting of the time t decay of the normalized PL intensity I/I_0 to the stretched exponential function, $I/I_0 = \exp[-(t/\tau)^{\beta}]$, where τ is the PL decay constant and β ($0 < \beta \leq 1$) is the stretched exponent, yielded $\tau \cong 252$ µs and $\beta \cong 0.83$ for the Al-codoped glass, and $\tau \cong 18$ µs and $\beta \cong 0.68$ for the Al-free glass. The stretched exponent β represents the degree of the distribution in τ; there is no distribution at $\beta = 1$ and the distribution becomes large as β decreases. Thus, the site-to-site distribution of the local environment of Nd^{3+} ions in the Al-codoped glass is smaller than that in the Al-free glass.

Theoretical PL decay constants of the glasses obtained in this study were evaluated using the Judd–Ofelt analysis.[36),37)] Inte-

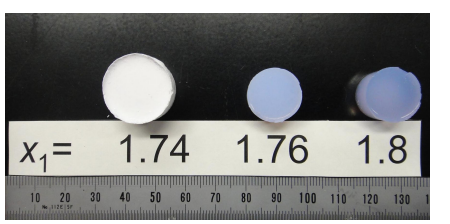

Fig. 1. (Color online) Effect of the amount of water added in the first mix (x_1) on the appearance of dried gels prepared using neodymium acetate as an RE salt at $z_{Al} = 0.01$.

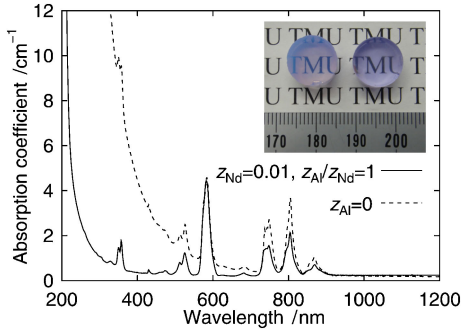

Fig. 2. (Color online) Optical absorption spectra of Nd-doped glasses prepared at $z_{Al}/z_{Nd} = 1$ (Al-codoped glass) and $z_{Al} = 0$ (Al-free glass). A photograph of the Al-codoped (right) and Al-free (left) glasses is shown too.

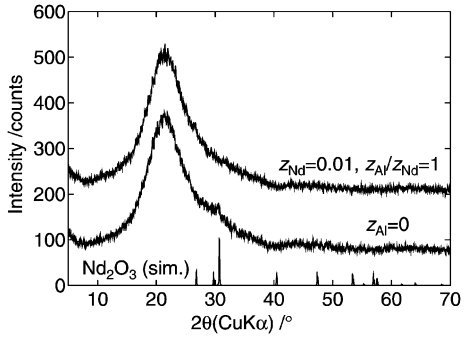

Fig. 3. XRD patterns of crushed Nd-doped glasses prepared at $z_{Al}/z_{Nd} = 1$ (Al-codoped glass) and $z_{Al} = 0$ (Al-free glass). The data were taken at intervals of 0.02°, and averaged over five adjacent points for visibility. Simulated pattern of Nd_2O_3 (space group $P\bar{3}m1$, $a = 3.831$Å, $c = 5.999$Å), calculated by RIETAN-FP,[45)] is also shown.

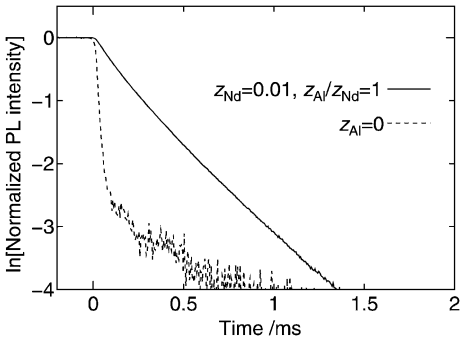

Fig. 4. PL decay curves of the $^4F_{3/2} \rightarrow {}^4I_{11/2}$ transition of Nd^{3+} ions in glasses prepared at $z_{Al}/z_{Nd} = 1$ (Al-codoped glass) and $z_{Al} = 0$ (Al-free glass).

grated intensity of each absorption band of Nd^{3+} ions due to the 4f–4f electron dipole transition is represented by

$$\frac{1}{\bar{\lambda}_{abs}} \int_{band} \sigma d\lambda = \frac{1}{4\pi\varepsilon_0} \frac{8\pi^3 e^2}{3hc(2J'+1)} \frac{(n^2+2)^2}{9n} S, \quad (1)$$

where $\bar{\lambda}_{abs}$ is average wavelength of the relevant absorption band, σ is optical absorption cross-section, ε_0 is the vacuum permittivity, e is the elementary charge, c is the speed of light, h is the Plank constant, n is the refractive index, and $2J'+1$ is the multiplicity of the lower level. The line strength S was independently determined for nine groups of absorption bands between 400 and 920 nm[7] employing n of undoped silica glass,[38] and was substituted into the expression for the transition from the lower level bJ' to the upper level aJ,

$$S = \sum_{t=2,4,6} \Omega_t |\langle aJ \| U^{(t)} \| bJ' \rangle|^2. \quad (2)$$

The resultant nine linear equations were solved to derive three common intensity parameters Ω_t ($t = 2, 4, 6$), which were further used to calculate the emission probability A from the upper level aJ to the lower level bJ',

$$A(aJ \rightarrow bJ') = \frac{1}{4\pi\varepsilon_0} \frac{64\pi^4 e^2}{3h\bar{\lambda}_{em}^3(2J+1)} \frac{n(n^2+2)^2}{9} \times \sum_{t=2,4,6} \Omega_t |\langle bJ' \| U^{(t)} \| aJ \rangle|^2, \quad (3)$$

where $\bar{\lambda}_{em}$ is the peak wavelength of the relevant emission band. The unit tensor operators $|\langle aJ \| U^{(t)} \| bJ' \rangle|^2 = |\langle bJ' \| U^{(t)} \| aJ \rangle|^2$ ($t = 2, 4, 6$) were taken from refs.[39),40)] The theoretical PL decay constant τ_{JO} is expressed by

$$\tau_{JO} = \frac{1}{\sum_{J'} A(aJ \rightarrow bJ')}. \quad (4)$$

The obtained Ω values were substituted into Eq. (2) to derive calculated line strength S_c. The quality of the least squares optimization of the Ω values can be expressed using the root mean square (rms) deviations in S and $S_c - S$ as $[\sum_i (S_{c,i} - S_i)^2 / \sum_i S_i^2]^{1/2}$,[41] where subscript i denotes the index of absorption bands involved in this calculation. The results of the Judd–Ofelt analysis are summarized in **Table 1**. The PL quantum yield Φ was calculated from the ratio of the experimental and theoretical PL decay constants as

$$\Phi = \frac{k_r}{k_r + k_{nr}} = k_r \tau_{exp} = \frac{\tau_{exp}}{\tau_{JO}}, \quad (5)$$

where k_r and k_{nr} are the radiative and nonradiative rate constants, respectively.

Table 1. Results of Judd–Ofelt analysis, theoretical lifetime, observed PL decay constants, and SiOH concentrations of Nd-doped glasses prepared at $z_{Al}/z_{Nd} = 1$ (Al-codoped glass) and $z_{Al} = 0$ (Al-free glass)

z_{Al}	z_{Nd}	Intensity parameters (10^{-20} cm^2)			PL decay constants (μs)		$\frac{\tau_{exp}}{\tau_{JO}}$	SiOH concentrations (10^{20} cm^{-3})
		Ω_2	Ω_4	Ω_6	τ_{exp}	τ_{JO}		
0	0.01	2.9	3.5	4.0	18	559	0.03	2.2
0.01	0.01	5.5	3.1	2.8	252	717	0.35	2.0

4. Discussion

As shown in Fig. 2, visible and ultraviolet transparency of the Al-free glass is not good due to light scattering. This sample contains Nd_2O_3 crystallites (Fig. 3), and similar results have also been reported in several Nd-doped silica glasses.[6),14)] However, the diffraction peak shown in Fig. 3 is weak and relatively broad, suggesting that the average size of the crystallites is too small to account for the light scattering. Thus, the low transparency of the Al-free glass is likely due to the precipitation of Nd-rich phases of much larger sizes.[18)] The Nd_2O_3 crystallites may be formed by the partial crystallization of the Nd-rich phases. Figure 4 shows that PL decay of the Al-free glass is much faster than that of Al-codoped glass. The fast PL decay of the Al-free glass is attributable to the aggregation of Nd^{3+} ions and the resultant concentration quenching, supporting the model that Nd^{3+} ions are concentrated in the Nd-rich phases in the Al-free glass. In contrast, the increase in β with the Al codoping corresponds to an increase in the homogeneity of the local environment of Nd^{3+} ions in the Al-codoped glass. These observations indicate that the enhancement of the dissolution of Nd^{3+} ions results in the good transparency of the Al-codoped glass, as has also been pointed out in many previous studies.[3)–18)]

Table 1 lists results of the Judd–Ofelt analysis for Al-free and Al-codoped glasses. In both samples the relative rms deviation in the S values was ~5%. The error due to the elution of Nd^{3+} ions is taken into account, and that due to the difference of refractive index between the pure silica glass and the samples (~0.005[34)]) is insignificant. Thus, the uncertainty in the intensity parameters may be less than ±20%, although it would be larger in the Al-codoped glass because of the possible elusion loss of Al^{3+} ions, which was not considered in this study. The Al codoping increases the Ω_2 value, suggesting increases in the asymmetry around Nd^{3+} ions and the covalency of Nd–O bonds.[42),43)] In contrast, the Ω_4 and Ω_6 values are decreased, and it is an indication that Nd–O bonds become more covalent.[44)] These changes are consistent with previous reports.[7),17)]

The τ_{JO} values for the $^4F_{3/2} \rightarrow {}^4I_{11/2}$ transition of Nd^{3+} ions obtained by the Judd–Ofelt analysis in this study are a bit larger than those reported for other Nd-doped (371,[3)] 348–360 μs[7)]) and Nd–Al codoped (495,[3)] 485–572,[7)] 640,[12)] 507–538,[17)] and 806 μs[26)]) glasses, although the reason is currently unclear. The small Φ value of the Al-free glass (~0.03) is due to the large discrepancy between the τ_{exp} and τ_{JO} values. The τ_{exp} value of the Al-codoped glass is much larger than that of the Al-free glass because of the enhanced dispersion of Nd^{3+} ions, resulting in a relatively large Φ value (~0.3–0.4). However, the τ_{exp} value is not large enough, as compared with PL decay constants reported for Nd–Al codoped glasses (280–450,[3),4)] 257–425,[7)] 250–550,[12)] 325,[14)] 240–250,[17)] and 376 μs[27)]). It is partly because of the small z_{Al}/z_{Nd} value ($z_{Al}/z_{Nd} = 1$). Most of

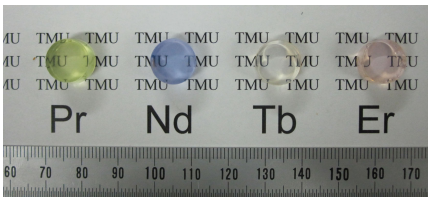

Fig. 5. (Color online) Photograph of various RE-doped silica glasses prepared at $z_{RE} = 0.01$ and $z_{Al}/z_{RE} = 1$.

the Nd–Al codoped glasses reported so far have been prepared at larger z_{Al}/z_{Nd} values, typically at ~3–20. It has also been reported for Nd–Al codoped silica glasses prepared by CVD method that the PL intensity increases with an increase in z_{Al}/z_{Nd} upto $z_{Al}/z_{Nd} \cong 10$.[4] Thus, $z_{Al}/z_{Nd} = 1$ may not be sufficient to disperse Nd^{3+} ions completely. Another probable reason is the high concentration of SiOH groups ($\sim 2 \times 10^{20}\,cm^{-3}$), which commonly accelerate the nonradiative transition of PL centers. In Nd-doped silica glasses, PL decay constants as large as ~400–500 μs have been realized by hydrogen-free synthesis using the plasma CVD technique,[4] and by H–D isotope exchange of SiOH groups to decrease the phonon energy of the relevant stretching mode.[7]

5. Conclusions

Monolithic transparent rare-earth (RE) and aluminum (Al) codoped silica glasses have been prepared by a cosolvent-free sol–gel process that produces macroporous gels. Al codoping increases the transparency of Nd-doped silica glasses. It also increases the quantum yield of infrared photoluminescence of Nd^{3+} ions. These observations indicate that the Al codoping enhances the dissolution of Nd^{3+} ions and suppresses the concentration quenching. **Figure 5** shows silica glasses doped by several different RE ions, illustrating the usefulness of this technique to prepare monolithic transparent RE-doped silica glasses.

Acknowledgments This work was partly supported by the Nippon Sheet Glass Foundation for Materials Science and Engineering, and a Grant-in-Aid for Scientific Research (B) (No. 24350109) from the Japan Society for the Promotion of Science (JSPS).

References

1) "Rare-Earth-Doped Fiber Lasers and Amplifers", 2nd ed., Ed. by M. J. F. Digonnet, Marcel Dekker, New York (2001).
2) M. J. Weber, *J. Non-Cryst. Solids*, **123**, 208–222 (1990).
3) Y. Ishii, H. Namikawa, K. Arai, A. Noda, A. Negishi and T. Handa, *Yogyo-Kyokai-Shi*, **93**, 498–504 (1985).
4) K. Arai, H. Namikawa, K. Kumata and T. Honda, *J. Appl. Phys.*, **59**, 3430–3436 (1986).
5) A. J. Berry and T. A. King, *J. Phys. D: Appl. Phys.*, **22**, 1419–1422 (1989).
6) T. Fujiyama, M. Hori and M. Sasaki, *J. Non-Cryst. Solids*, **121**, 273–278 (1990).
7) I. M. Thomas, S. A. Payne and G. D. Wilke, *J. Non-Cryst. Solids*, **151**, 183–194 (1992).
8) S. Sen and J. F. Stebbins, *J. Non-Cryst. Solids*, **188**, 54–62 (1995).
9) M. J. Lochhead and K. L. Bray, *Chem. Mater.*, **7**, 572–577 (1995).
10) M. Nogami and Y. Abe, *J. Non-Cryst. Solids*, **197**, 73–78 (1996).
11) Y. Zhou, Y. L. Lam, S. S. Wang, H. L. Liu, C. H. Kam and Y. C. Chan, *Appl. Phys. Lett.*, **71**, 587–589 (1997).
12) A. Martinez, L. A. Zenteno and J. C. K. Kuo, *Appl. Phys. B*, **67**, 17–21 (1998).
13) S. Sen, S. B. Orlinskii and R. M. Rakhmatullin, *J. Appl. Phys.*, **89**, 2304–2308 (2001).
14) M. Langlet, C. Coutier, W. Meffre, M. Audier, J. Fick, R. Rimet and B. Jacquier, *J. Lumin.*, **96**, 295–309 (2002).
15) A. Monteil, S. Chaussedent, G. Alombert-Goget, N. Gaumer, J. Obriot, S. J. L. Ribeiro, Y. Messaddeq, A. Chiasera and M. Ferrari, *J. Non-Cryst. Solids*, **348**, 44–50 (2004).
16) A. Saitoh, S. Matsuishi, C. Se-Weon, J. Nishii, M. Oto, M. Hirano and H. Hosono, *J. Phys. Chem. B*, **110**, 7617–7620 (2006).
17) Y. Qiao, N. Da, D. Chen, Q. Zhou, J. Qiu and T. Akai, *Appl. Phys. B*, **87**, 717–722 (2007).
18) B. Hatta and M. Tomozawa, *J. Non-Cryst. Solids*, **354**, 3184–3193 (2008).
19) C. J. Brinker and G. W. Scherer, "Sol–Gel Science, The Physics and Chemistry of Sol–Gel Processing", Academic Press, New York (1990).
20) R. D. Shoup, in "Ultrastructure Processing of Advanced Ceramics", Ed. by J. D. Mackenzie, D. R. Ulrich, Wiley, New York (1988) pp. 347–354.
21) E. M. Rabinovich, D. W. Johnson, Jr., J. B. MacChesney and E. M. Vogel, *J. Am. Ceram. Soc.*, **66**, 683–688 (1983).
22) E. M. Rabinovich, J. B. MacChesney, D. W. Johnson, Jr., J. R. Simpson, B. W. Meagher, F. V. Dimarcello, D. L. Wood and E. A. Sigety, *J. Non-Cryst. Solids*, **63**, 155–161 (1984).
23) G. W. Scherer and J. C. Luong, *J. Non-Cryst. Solids*, **63**, 163–172 (1984).
24) R. Clasen, *J. Non-Cryst. Solids*, **89**, 335–344 (1987).
25) M. Toki, S. Miyashita, T. Takeuchi, S. Kanbe and A. Kochi, *J. Non-Cryst. Solids*, **100**, 479–482 (1988).
26) Y. Fujimoto and M. Nakatsuka, *J. Non-Cryst. Solids*, **215**, 182–191 (1997).
27) T. Sato, Y. Fujimoto, H. Okada, H. Yoshida, M. Nakatsuka, T. Ueda and A. Fujinoki, *Appl. Phys. Lett.*, **90**, 221108 (2007).
28) K. Kajihara, M. Hirano and H. Hosono, *Chem. Commun. (Camb.)*, 2580–2582 (2009).
29) K. Kajihara, S. Kuwatani, R. Maehana and K. Kanamura, *Bull. Chem. Soc. Jpn.*, **82**, 1470–1476 (2009).
30) S. Kuwatani, R. Maehana, K. Kajihara and K. Kanamura, *Chem. Lett.*, **39**, 712–713 (2010).
31) K. Kajihara, S. Kuwatani and K. Kanamura, *Appl. Phys. Express*, **5**, 012601 (2012).
32) M. Yamane, S. Aso, S. Okano and T. Sakaino, *J. Mater. Sci.*, **14**, 607–611 (1979).
33) T. Kawaguchi, H. Hishikura, J. Iura and Y. Kokubu, *J. Non-Cryst. Solids*, **63**, 61–69 (1984).
34) H. Namikawa, K. Arai, K. Kumata, Y. Ishii and H. Tanaka, *Jpn. J. Appl. Phys.*, **21**, L360–L362 (1982).
35) K. M. Davis, A. Agarwal, M. Tomozawa and K. Hirao, *J. Non-Cryst. Solids*, **203**, 27–36 (1996).
36) B. R. Judd, *Phys. Rev.*, **127**, 750–761 (1962).
37) G. S. Ofelt, *J. Chem. Phys.*, **37**, 511–520 (1962).
38) B. Brixner, *J. Opt. Soc. Am.*, **57**, 674–676 (1967).
39) W. T. Carnall, P. R. Fields and K. Rajnak, *J. Chem. Phys.*, **49**, 4424–4442 (1968).
40) W. F. Krupke, *IEEE J. Quantum Electron.*, **QE-10**, 450–457 (1974).
41) W. F. Krupke, *IEEE J. Quantum Electron.*, **QE-7**, 153–159 (1971).
42) R. Reisfeld, *J. Electrochem. Soc.*, **131**, 1360–1364 (1984).
43) S. Tanabe, T. Ohyagi, N. Soga and T. Hanada, *Phys. Rev. B*, **46**, 3305–3310 (1992).
44) S. Tanabe, T. Hanada, T. Ohyagi and N. Soga, *Phys. Rev. B*, **48**, 10591–10594 (1993).
45) F. Izumi and K. Momma, *Solid State Phenom.*, **130**, 15–20 (2007).